JOURNAL OF NATURAL PRODUCTS

Article

pubs.acs.org/jnp

Identification of Compounds with Efficacy against Malaria Parasites from Common North American Plants

Shengxin Cai,[†,‡,#] April L. Risinger,[§,⊥,#] Shalini Nair,[∥] Jiangnan Peng,[§] Timothy J. C. Anderson,[∥] Lin Du,[†,‡] Douglas R. Powell,[†] Susan L. Mooberry,*[,§,⊥] and Robert H. Cichewicz*[,†,‡]

[†]Department of Chemistry and Biochemistry, Stephenson Life Sciences Research Center, and [‡]Natural Products Discovery Group, and Institute for Natural Products Applications and Research Technologies, University of Oklahoma, Norman, Oklahoma 73019, United States

[§]Department of Pharmacology and [⊥]Cancer Therapy and Research Center, University of Texas Health Science Center, San Antonio, Texas 78229, United States

[∥]Department of Genetics, Texas Biomedical Research Institute, San Antonio, Texas 78227, United States

Supporting Information

ABSTRACT: Some of the most valuable antimalarial compounds, including quinine and artemisinin, originated from plants. While these drugs have served important roles over many years for the treatment of malaria, drug resistance has become a widespread problem. Therefore, a critical need exists to identify new compounds that have efficacy against drug-resistant malaria strains. In the current study, extracts prepared from plants readily obtained from local sources were screened for activity against *Plasmodium falciparum*. Bioassay-guided fractionation was used to identify 18 compounds from five plant species. These compounds included eight lupane triterpenes (**1**−**8**), four kaempferol 3-*O*-rhamnosides (**10**−**13**), four kaempferol 3-*O*-glucosides (**14**−**17**), and the known compounds amentoflavone and knipholone. These compounds were tested for their efficacy against multi-drug-resistant malaria parasites and counterscreened against HeLa cells to measure their antimalarial selectivity. Most notably, one of the new lupane triterpenes (**3**) isolated from the supercritical extract of *Buxus sempervirens*, the common boxwood, showed activity against both drug-sensitive and -resistant malaria strains at a concentration that was 75-fold more selective for the drug-resistant malaria parasites as compared to HeLa cells. This study demonstrates that new antimalarial compounds with efficacy against drug-resistant strains can be identified from native and introduced plant species in the United States, which traditionally have received scant investigation compared to more heavily explored tropical and semitropical botanical resources from around the world.

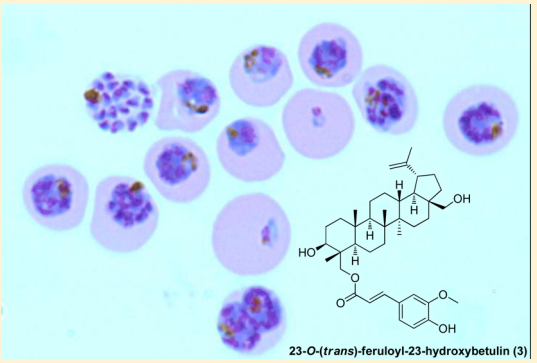

In 2013, malaria infections impacted an estimated 198 million people across 97 different countries, resulting in an estimated 584 000 deaths.[1] While several related *Plasmodium* spp. are implicated in the disease, *Plasmodium falciparum* is responsible for the majority of deaths. No effective vaccine has been developed for malaria, which has meant that small-molecule therapeutics must continue to fulfill the treatment needs of infected patients and at-risk individuals. There are four major classes of compounds that are used clinically to treat malaria: (1) quinolines (e.g., chloroquine, quinine, mefloquine), (2) antifolates (e.g., sulfadoxine, pyrimethamine), (3) artemisinin derivatives (e.g., artesunate, artemether), and (4) antimicrobials (e.g., doxycycline); however, resistance to the most widely used agents from the first three major drug classes is now widespread.[2] Specifically, resistance to artemisinin derivatives, which form the basis of widely used combination therapies for malaria, is now common across Southeast Asia.[3] The further spread of artemisinin resistance is anticipated to be disastrous for malaria control efforts.[4] It is therefore imperative that new classes of drugs be developed for the treatment of this infectious organism. While several promising new antimalarial compounds are being explored,[5,6] the high rate of attrition for candidate molecules under clinical investigation suggests that additional efforts are needed to develop alternative therapeutic strategies.

The majority of approved treatment options for malaria are either plant-derived natural products or synthetic analogues of plant-derived compounds. Quinine, originally obtained from the bark of the South American cinchona tree, was introduced to Europe in the 17th century as an antimalarial treatment by Jesuit priests returning from Peru.[7] Chloroquine has been widely used for over 50 years before resistance became widespread. Artemisinin, derived from sweet wormwood (*Artemisia annua*), clears parasites from the blood of patients

Special Issue: Special Issue in Honor of John Blunt and Murray Munro

Received: October 1, 2015

DOI: 10.1021/acs.jnatprod.5b00874
J. Nat. Prod. XXXX, XXX, XXX−XXX

Chart 1

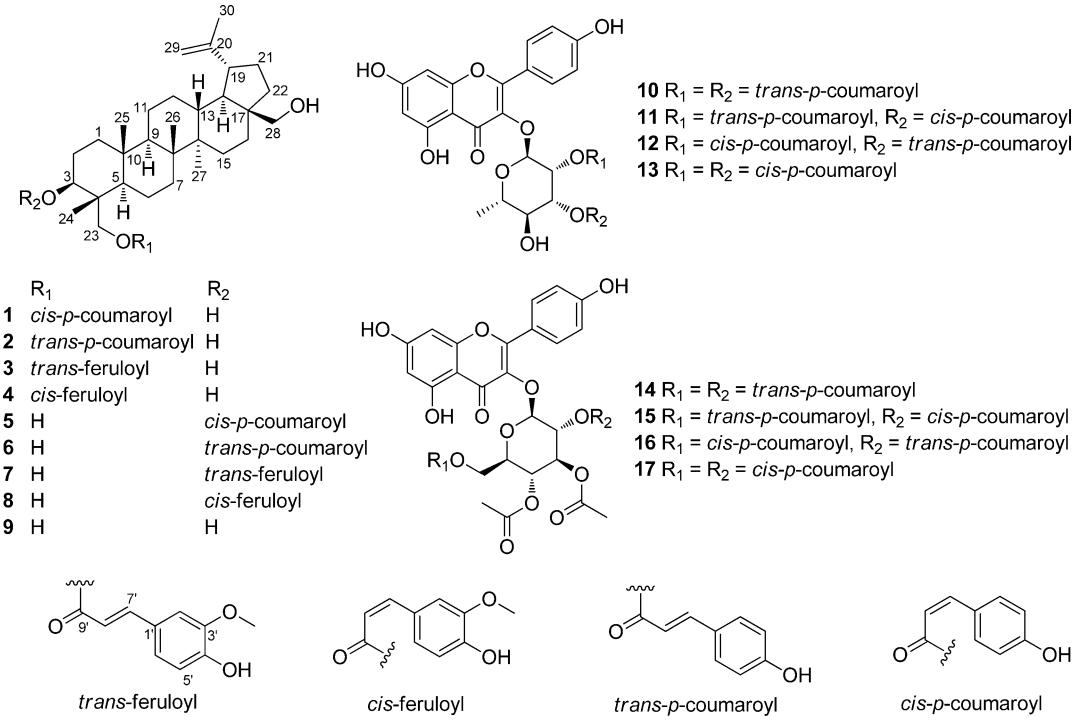

more rapidly than any other known antimalarial.[8] Artemisinin derivatives are now widely used as part of combination therapies with other drugs such as lumefantrine or mefloquine. Even atovaquone, which is combined with proguanil in the drug Malarone, is an analogue of the plant-derived compound lapachol from *Tabebuia* sp. (Bignoniaceae). The recent identification of the alkaloid tazopsine from a Madagascan plant (*Strychnopsis thousarsii*), which kills the liver stage of malaria, further supports the continued exploration of plants for antimalarial leads.[9] Despite these successes, only a small fraction of the world's plant species have been screened for antimalarial activity. Furthermore, the plants that have been tested tend to have been obtained solely from the flora of malaria-endemic countries or have been selected based on a history of medicinal use against the disease.[10,11]

The intent of this study was to expand the diversity of plants tested for bioactive compounds that are active against malaria by focusing on readily available botanical resources from our local environment in the south-central United States. Specifically, we have focused exclusively on plants that grow well in the sometimes harsh environment of southern Texas.[12] Our studies have yielded several potent and selective inhibitors of drug-resistant *P. falciparum*, which highlight the value of local North American plants as a resource for bioactive natural product leads for malaria.

RESULTS AND DISCUSSION

A collection of 1281 plant extracts was generated from 463 species of plants that grow in Texas, USA. The extracts were generated using supercritical fluid (CO_2) extraction with or without methanol, as well as traditional aqueous extractions to capture as broad a range of metabolites as possible from each sample. For the initial screening, extracts were tested for their abilities to inhibit the growth of the drug-sensitive HB3 strain of *P. falciparum* at a concentration of 20 μg/mL. Using this delimiting parameter, five extracts were prioritized for bioassay-guided fractionation based on their capacity to specifically inhibit the growth of the malaria parasite with minimal or no toxicity toward human cells. It is worth noting the important role that the extraction methods played in liberating the active compounds from the freeze-dried plant material; among the hits, only a single extract from a given plant yielded a bioactive hit. In other words, the different extraction methods performed on a given plant captured unique sets of metabolites that were distinct enough from one another so as to preclude the possibility that a single extraction method would have sufficed to produce the hits detected in this project.

Our investigation of the compounds responsible for the antimalarial activities of the active extracts was led by an HPLC-based microtiter plate fractionation process[13] in which approximately 5 mg of extract was separated into 92 wells of a 96-well plate. The fractions were split with half the material used for bioassay testing, and the other half was retained for LCESIMS analysis of the active wells. This approach enabled us to use the LCESIMS data to rapidly guide the follow-up metabolite purification process. We used this tactic to purify a total of 18 compounds that exhibited varying degrees of antimalarial activity, including knipholone,[14] amentoflavone,[15] eight lupane triterpenes [**1**−**8**; compounds **3**−**5** and **7**−**8** are new, whereas **1** (23-*O*-(*Z*)-*p*-coumaroyl-23-hydroxybetulin), **2** (23-*O*-(*E*)-*p*-coumaroyl-23-hydroxybetulin), and **6** (3-*O*-(*E*)-*p*-coumaroyl-23-hydroxybetulin) were reported earlier this year by the Kinghorn group],[16] four known kaempferol 3-*O*-rhamnosides (**10**−**13**),[17] and four known kaempferol 3-*O*-glucosides (**14**−**17**).[18−20]

Eight lupane triterpenes (**1**−**8**, of which **3**−**5** and **7**−**8** are new analogues) were purified from the methanolic supercritical extract of the common boxwood, *Buxus sempervirens* L. (Buxaceae), after their detection using our microtiter plate fractionation process. Compound **1** was obtained as colorless, block-shaped crystals, and its molecular formula was established as $C_{39}H_{56}O_5$ based on HRESIMS data. The planar structure of

DOI: 10.1021/acs.jnatprod.5b00874
J. Nat. Prod. XXXX, XXX, XXX−XXX

Table 1. ^{1}H NMR Spectroscopic Data for Compounds 1, 3–5, 7, and 8 (δ in ppm, J in Hz)

no.	1[a,b]	3[c,d]	4[c,d]	5[a,d]	7[c,d]	8[c,d]
1	1.50, m	1.74, m	1.63, m	1.60, m	1.73, m	1.73, m
	0.75, m	1.00, m	0.83, m	0.88, m	1.02, m	1.02, m
2	1.45, m	1.67, m	1.58, m	1.67, m	1.76, m	1.76, m
				1.59, m		
3	3.29, dd (9.6, 6.0)	3.61, dd (4.9, 11.2)	3.46, dd (5.2, 11.8)	4.78, dd (5.0, 11.8)	4.95, m	4.90, m
5	0.86, m	1.20, m	0.95, m	1.21, m	1.32, m	1.32, m
6	1.25, m	1.46, m	1.35, m	1.40, m	1.48, m	1.48, m
				1.28, m		
7	1.12, m	1.41, m	1.45, m	1.42, m	1.60, m	1.60, m
	1.06, m		1.20, m	1.27, m	1.38, m	1.38, m
9	1.12, m	1.40, m	1.23, m	1.31, m	1.44, m	1.44, m
11	1.29, m	1.46, m	1.40, m	1.35, m	1.45, m	1.45, m
	1.12, m			1.16, m		
12	1.55, m	1.70, m	1.65, m	1.60, m	1.69, m	1.69, m
	0.95, m					
13	1.54, m	1.70, m	1.66, m	1.60, m	1.68, m	1.68, m
15	1.55, m	1.76, m	1.58, m	1.68, m	1.78, m	1.78, m
	0.78, m	1.01, m	0.91, m	0.91, m	1.05, m	1.05, m
16	1.85, m	1.92, m	1.92, m	1.90, m	1.96, m	1.96, m
	0.98, m	1.14, m	1.12, m	1.05, m	1.19, m	1.19, m
18	1.42, m	1.58, t (11.7)	1.57, t (11.5)	1.48, t (11.8)	1.61, m	1.61, m
19	2.33, m	2.41, m	2.41, m	2.39 m	2.42, m	2.42, m
21	1.83, m	1.95, m	1.92, m	1.85, m	1.95, m	1.95, m
	1.23, m	1.37, m	1.33, m	1.25, m	1.35, m	1.35 m,
22	1.83, m	1.89, m	1.90, m	1.84, m	1.91, m	1.91, m
	0.85, m	0.99, m	0.98, m	0.88, m	0.99, m	0.99, m
23	3.91, d (11.5)	4.09, d (11.4)	4.08, d (11.4)	3.11, d (10.9)	3.32[e]	3.28[e]
	3.87, d (11.5)	4.04, d (11.4)	3.99, d (11.4)	2.93, d (10.9)	3.14, d (12.0)	3.10, d (11.5)
24	0.60, s	0.77, s	0.73, s	0.57, s	0.80, s	0.66, s
25	0.75, s	0.92, s	0.87, s	0.82, s	0.95, s	0.92, s
26	0.91, s	1.08, s	1.03, s	0.98, s	1.09, s	1.08, s
27	0.74, s	0.97, s	0.83, s	0.94, s	1.04, s	1.04, s
28	3.47, d (10.7)	3.73, d (10.4)	3.72, d (10.8)	3.51, d (10.8)	3.74, d (11.5)	3.74, d (11.5)
	3.04, d (10.7)	3.27, d (11.1)	3.27, d (10.8)	3.07, d (10.8)	3.29[e]	3.29[e]
29	4.63, d (2.3)	4.68, d (2.2)	4.68, d (2.2)	4.66, d (2.0)	4.69, brs	4.69, brs
	4.51, brs	4.57, brs	4.57, brs	4.53, brs	4.57, brs	4.57, brs
30	1.60, s	1.68, s	1.69, s	1.64, s	1.70, s	1.70, s
2′	7.57, d (8.7)	7.21, d (1.9)	7.66, d (2.0)	7.62, d (8.7)	7.18, d (1.8)	7.73, d (1.9)
3′	6.72, d (8.7)			6.73, d (8.7)		
5′	6.72, d (8.7)	6.83, d (8.2)	6.77, d (8.2)	6.73, d (8.7)	6.80, d (8.2)	6.75, d (8.2)
6′	7.57, d (8.7)	7.08, dd (8.3, 1.9)	7.08, dd (2.0, 8.3)	7.62, d (8.7)	7.05, dd (8.3, 1.8)	7.08, dd (8.2, 1.9)
7′	6.82, d (12.9)	7.63, d (15.9)	6.89, d (12.9)	6.80, d (13.0)	7.57, d (15.9)	6.84, d (12.8)
8′	5.75, d (12.9)	6.38, d (15.9)	5.81, d (12.8)	5.71, d (12.8)	6.33, d (15.9)	5.75, d (12.9)
OH-4′	9.82, s			9.34, brs		
OMe-3′		3.91, s	3.88, s		3.89, s	3.87, s

[a]Solvent was DMSO-d_6. [b]Performed on a 400 MHz Varian instrument. [c]Solvent was MeOH-d_4. [d]Performed on a 500 MHz Varian instrument. [e]Signal was overlapped with solvent peak.

compound **1** was determined by de novo analysis of its NMR data (Tables 1 and 2 and Figure 1) and, later, by comparing its NMR data to structurally related metabolites.[16] The relative configuration of the compound was determined based on ROESY experimental data (Figure 1), which were consistent with reported lupane triterpene analogues.[16] During the course of the NMR studies, we obtained crystals of compound **1** that were suitable for X-ray crystallography, which served to confirm the compound's planar structure, as well as its relative configuration (Figure 2). The absolute configuration of **1** was determined by refinement of the Hooft parameter.[21] To further substantiate the absolute configuration of the metabolite, compound **1** was hydrolyzed overnight in 1 M NaOH at room temperature, and the triterpene portion of the molecule (23-hydroxybetulin [**9**]) was purified from the hydrolysate. NMR (Figures S45 and S46, Supporting Information) and optical rotation ($[\alpha]^{20}_{D}$ +16) data obtained for the hydrolysis product were consistent with that reported for **9** ($[\alpha]^{20}_{D}$ +22).[22] The proposed absolute configuration is consistent with an in silico derived specific rotation value for **9** (calcd +68).[23,24]

Compound **2** was obtained as a white, amorphous powder, and the planar structure was determined by comparing its HRESIMS and NMR data with published data.[16] The relative

DOI: 10.1021/acs.jnatprod.5b00874
J. Nat. Prod. XXXX, XXX, XXX−XXX

Table 2. ^{13}C NMR Spectroscopic Data for Compounds 1, 3−5, 7, and 8

no.	1[a,b]	3[b,c]	4[b,c]	5[a,b]	7[c,d]	8[c,d]
1	38.4 CH_2	38.4 CH_2	38.2 CH_2	38.1 CH_2	37.9 CH_2	37.9 CH_2
2	27.1 CH_2	26.1 CH_2	26.0 CH_2	23.1 CH_2	22.9 CH_2	22.9 CH_2
3	70.4 CH	71.3 CH	71.1 CH	74.2 CH	74.4 CH	74.2 CH
4	41.9 C	41.9 C	41.7 C	41.5 C	41.6 C	41.6 C
5	47.7 CH	47.8 CH	47.2 CH	46.6 CH	46.5 CH	46.5 CH
6	18.2 CH_2	17.9 CH_2	17.9 CH_2	17.6 CH_2	17.3 CH_2	17.3 CH_2
7	33.9 CH_2	33.7 CH_2	33.7 CH_2	33.7 CH_2	33.3 CH_2	33.3 CH_2
8	40.9 C	40.7 C	40.6 C	40.8 C	40.6 C	40.6 C
9	50.5 CH	50.7 CH	50.4 CH	50.1 CH	50.3 CH	50.3 CH
10	36.9 C	36.7 C	36.6 C	36.7 C	36.5 C	36.5 C
11	20.8 CH_2	20.6 CH_2	20.5 CH_2	20.8 CH_2	20.6 CH_2	20.6 CH_2
12	25.3 CH_2	25.2 CH_2	25.1 CH_2	25.2 CH_2	25.1 CH_2	25.1 CH_2
13	37.2 CH	37.3 CH	37.2 CH	37.1 CH	37.2 CH	37.2 CH
14	42.5 C	42.4 C	42.3 C	42.7 C	42.4 C	42.4 C
15	26.9 CH_2	26.7 CH_2	26.5 CH_2	27.1 CH_2	26.7 CH_2	26.7 CH_2
16	29.5 CH_2	28.9 CH_2	28.9 CH_2	29.5 CH_2	28.9 CH_2	28.9 CH_2
17	47.9 C	47.5 C	47.5 C	47.8 C	47.8 C	47.8 C
18	48.6 CH	48.6 CH	48.5 CH	48.6 CH	48.5 CH	48.5 CH
19	47.8 CH	47.7 CH	47.7 CH	47.7 CH	47.9 CH	47.9 CH
20	150.9 C	150.4 C	150.4 C	150.8 C	150.3 C	150.3 C
21	29.8 CH_2	29.4 CH_2	29.4 CH_2	29.7 CH_2	29.4 CH_2	29.4 CH_2
22	34.3 CH_2	33.6 CH_2	33.6 CH_2	34.3 CH_2	33.7 CH_2	33.7 CH_2
23	65.6 CH_2	65.3 CH_2	65 CH_2	63.1 CH_2	63.1 CH_2	63.1 CH_2
24	12.6 CH_3	11.1 CH_3	11.1 CH_3	13.6 CH_3	12.3 CH_3	12.1 CH_3
25	16.7 CH_3	15.6 CH_3	15.5 CH_3	16.7 CH_3	15.6 CH_3	15.6 CH_3
26	16.2 CH_3	15.1 CH_3	15.0 CH_3	16.1 CH_3	15.1 CH_3	15.1 CH_3
27	14.7 CH_3	13.8 CH_3	13.6 CH_3	14.9 CH_3	13.8 CH_3	13.8 CH_3
28	58.4 CH_2	58.9 CH_2	58.9 CH_2	58.3 CH_2	58.9 CH_2	58.9 CH_2
29	110.1 CH_2	108.8 CH_2	108.8 CH_2	110.1 CH_2	108.8 CH_2	108.8 CH_2
30	19.2 CH_3	17.8 CH_3	17.7 CH_3	19.2 CH_3	17.9 CH_3	17.9 CH_3
1′	126.0 C	126.2 C	126.8 C	125.9 C	126.2 C	126.3 C
2′	132.7 CH	110.2 CH	113.1 CH	132.9 CH	110.0 CH	113.3 CH
3′	115.4 CH	148.0 C	147.0 C	115.3 CH	148.0 C	147.0 C
4′	159.3 C	149.3 C	148.1 C	159.2 C	149.0 C	148.0 C
5′	115.4 CH	115.1 CH	114.4 CH	115.3 CH	115.0 CH	114.0 CH
6′	132.7 CH	122.8 CH	124.7 CH	132.9 CH	122.7 CH	124.9 CH
7′	142.9 CH	145.4 CH	142.9 CH	143.1 CH	145.0 CH	144.1 CH
8′	116.2 CH	114.1 CH	115.6 CH	116.6 CH	114.3 CH	115.8 CH
9′	166.7 C	167.7 C	167.1 C	166.1 C	167.7 C	166.6 C
OMe-3′		55.0 CH_3	54.9 CH_3		55.0 CH_3	55.0 CH_3

[a]Solvent was DMSO-d_6. [b]Performed on a 100 MHz Varian instrument. [c]Solvent was MeOH-d_4. [d]Carbon data were determined by a combination of ^{13}C (100 MHz), HSQC (500 MHz), and HMBC (500 MHz) experiments.

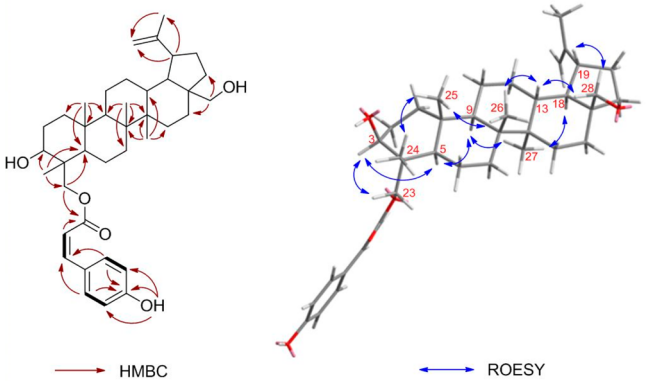

Figure 1. Key ^{1}H−^{1}H COSY, HMBC, and ROESY correlations for compound 1.

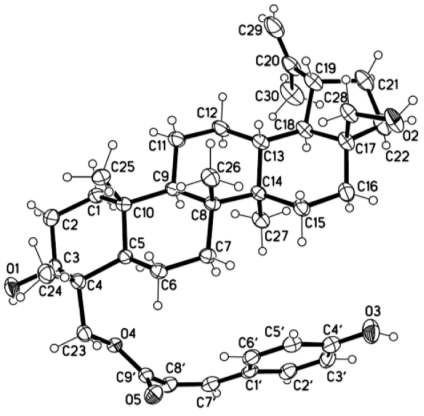

Figure 2. ORTEP structure generated from the X-ray diffraction data for a single crystal of 1.

DOI: 10.1021/acs.jnatprod.5b00874
J. Nat. Prod. XXXX, XXX, XXX−XXX

Table 3. Bioassay Data of Amentoflavone, Knipholone, and Compounds 1−17

compound	HB3 IC_{50} ± SE (μM)[a]	NHP1337 IC_{50} ± SE (μM)[a]	relative resistance (NHP1337/HB3)	HeLa IC_{50} ± SE (μM)[b]	fold selectivity (HeLa/HB3)	fold selectivity (HeLa/NHP1337)
amentoflavone	25 ± 2	19 ± 7	0.8	46.4 ± 0.4	1.9	2.4
knipholone	4.9 ± 0.6	5 ± 2	1.0	32.3 ± 0.3	6.6	6.5
1	0.8 ± 0.4	1.53 ± 0.04	1.9	7 ± 1	8.8	4.6
2	0.9 ± 0.1	0.85 ± 0.05	0.9	28 ± 3	31	33
3	0.5 ± 0.2	0.27 ± 0.03	0.5	>20	>40	>74
4 and **3** (3:1)	1.0 ± 0.1	0.31 ± 0.05	0.3	20 ± 4	20	65
5 and **6** (4:1)	2.3 ± 0.1	1.6 ± 0.1	0.7	22 ± 1	9.6	14
6	1.9 ± 0.2	1.4 ± 0.2	0.7	>20	>11	>14
7 and **8** (2:1)	3.0 ± 0.3	2.3 ± 0.4	0.8	>20	>6.7	>8.7
9	3.4 ± 0.5	5.2 ± 0.3	1.5	>20	>5.9	>3.8
10	0.6 ± 0.2	7 ± 1	12	20.6 ± 0.5	34	2.9
11	2.0 ± 0.6	4 ± 1	2.0	11.9 ± 0.7	6.0	3.0
12	0.50 ± 0.03	4.1 ± 0.5	8.2	9.3 ± 0.2	19	2.3
13	1.8 ± 0.4	7 ± 1	3.9	16 ± 1	8.9	2.3
14	0.6 ± 0.1	2.1 ± 0.6	3.5	<3	<5.0	<1.4
15	0.9 ± 0.2	5 ± 1	5.6	<3	<3.3	<0.6
16	0.8 ± 0.1	4 ± 1	5.0	<3	<3.8	<0.8
17	2.1 ± 0.9	3.8 ± 0.6	1.8	<3	<1.4	<0.8

[a]Inhibition of malaria parasites was evaluated using a SYBR green-based assay. [b]Inhibition of HeLa cells was evaluated using the sulforhodamine B assay.

configuration was confirmed using data from a ROESY experiment (Figure S1, Supporting Information). On the basis of these results, as well as biosynthetic considerations, the shared 23-hydroxybetulin scaffolds in **1** and **2** are presumed to possess the same absolute configurations.

Compound **3** was purified as a white, amorphous powder. HRESIMS indicated that this compound had the molecular formula $C_{40}H_{58}O_6$ ($[M - H]^-$ ion at m/z 633.4178, calcd 633.4161). NMR analysis revealed that **3** exhibited ^1H and ^{13}C NMR data (Tables 1 and 2) that were similar to **2** with the addition of proton (δ 3.91, 3H, s) and carbon (δ 55.0, CH_3) signals indicative of a new methoxy group. Further 2D NMR analysis confirmed the placement of the methoxy group on the aromatic ester moiety, thus establishing that **3** is a new *trans*-feruloyl-containing analogue of **2**.

Compound **4** was obtained as a mixture with compound **3** (ca. ∼3:1 ratio of **4**:**3**). It was observed by LCESIMS that **4** readily interconverted to **3** within several hours of its purification by HPLC. Therefore, structure determination of the metabolite proceeded using the compound mixture. Both compounds were found to bear the same molecular formula based on HRESIMS data. The 1D NMR data (Tables 1 and 2) indicated that the two components in the mixture were nearly identical, with the major difference being that the olefinic *trans*-coupled protons in **3** (J = 15.9 Hz) appeared to be *cis* configured (J = 12.9 Hz) in **4**. Subsequent 2D NMR analysis of **4** confirmed that the remainder of the compound was structurally identical to **3**. On the basis of these data, as well as their shared biogenic origin, the absolute configuration of the triterpene portions of both molecules were presumed to be identical. The *cis*−*trans* isomerization of **4** to **3** has precedence among other feruloyl-containing triterpene metabolites.[25,26] Both natural and laboratory-related factors are likely involved in the interconversion between these two geometric isomers. While our testing of the plant material remains incomplete, the available data suggest that both isomers might be present in the original plant tissues.

Compound **6**, which was very recently reported by the Kinghorn group and named 3-*O*-(*E*)-*p*-coumaroyl-23-hydroxybetulin, was isolated as a white, amorphous powder, and its structure determined by NMR spectroscopy (Table S1, Supporting Information) and HRESIMS, as well as by comparing its experimentally derived data to those published for structurally related metabolites.[16] The assignment of the position of the *trans*-*p*-coumaroyl group was based on an HMBC correlation from H-3 (δ 4.83 dd, 5.0, 11.2) to C-9′ (δ 166.6 C). Compound **5** was isolated as a mixture with **6** (ratio of **5**:**6**, ∼4:1). An analysis of its 1D and 2D NMR data (Tables 1 and 2 and Figure S3, Supporting Information) indicated that the difference between compounds **5** and **6** was also due to isomerization of an olefinic bond. The *trans*-configured coumaroyl group in compound **6** was replaced by a *cis*-configured coumaroyl group in **5** based on *J*-based analysis of the olefinic protons (J = 16.0 Hz in **6** versus J = 12.9 Hz in **5**). The *cis*-*p*-coumaroyl group was determined to be appended to the C-3 oxygen atom based on an HMBC correlation from H-3 (δ 4.78 dd, 5.0, 11.8) to C-9′ (δ 166.1 C).

Compounds **7** and **8** were also obtained as a mixture in a ∼2:1 ratio. The HRESIMS data revealed that these two compounds shared the same molecular formula ($C_{40}H_{58}O_6$). The ^1H and ^{13}C NMR data (Tables 1 and 2) indicated that both components in the mixture were structurally similar and contained the same lupane triterpene skeleton found in compounds **5** and **6**. The validity of this assessment was confirmed by a hydrolysis experiment, which yielded triterpene **9** from both metabolites. Subsequent 1D and 2D NMR analysis indicated that the major component, **7**, exhibited resonances characteristic for a *trans*-configured feruloyl group connected to the C-3 oxygen [HMBC correlation from H-3 (δ 4.95 m) to C-9′ (δ 167.7 C)]. Similarly, the less abundant component, **8**, contained a *cis*-configured feruloyl group connected to C-3.

The eight lupane triterpenes exhibited modest differences in their respective potencies (IC_{50} values ranging from 0.5 to 3.0 μM) against the drug-sensitive HB3 parasites (Table 3). This is consistent with a report published earlier this year, wherein it

DOI: 10.1021/acs.jnatprod.5b00874
J. Nat. Prod. XXXX, XXX, XXX−XXX

was disclosed that compounds **1**, **2**, and **6** were active against the drug-sensitive *P. falciparum* Dd2 strain at concentrations that were similar to those used in our experiments.[16] Notably, the most potent metabolite in our assay was the new compound **3**, which contains a *trans*-feruloyl group attached to the C-23 oxygen atom, with an IC_{50} of 0.5 μM against the HB3 parasite. Compared to **3**, compounds with structurally related moieties attached to the C-23 oxygen atom, including *cis*-feruloyl (**4**), *cis*-*p*-coumaroyl (**1**), and *trans*-*p*-coumaroyl (**2**) groups, also inhibited the parasite, but at slightly higher (2-fold greater) concentrations. In contrast, compounds containing these substituents on the C-3 oxygen were 4- to 6-fold less potent than **3**, indicating that modifications at this position had a less desirable influence on their biological profiles. Interestingly, it was noted that the absence of any feruloyl or coumaroyl groups resulting in the unadorned lupane triterpene **9** yielded a less potent inhibitor with an IC_{50} value of 3.4 μM.

The efficacies of the lupane triterpenes were also evaluated against a multi-drug-resistant clone of *P. falciparum* that was recently isolated from the Thailand−Myanmar border. Other than compounds **1** and **9**, the triterpenes were slightly more potent against the drug-resistant NHP1337 parasites as compared to the drug-sensitive HB3 strain (Table 3). Overall, the triterpene derivatives showed selective activities against the parasites versus human cells with compounds **2** and **3**, which contain *trans*-*p*-coumaroyl or *trans*-feruloyl groups, respectively, at C-23, having greater than 30-fold selectivity for both the drug-sensitive and drug-resistant parasites. The potency and selectivity of **3** against both drug-sensitive and -resistant parasites further supports that this class of compounds may be an interesting lead for exploiting as a new class of antimalarial agents that are chemically distinct from existing therapeutics.

Four known kaempferol 3-*O*-rhamnosides were isolated from the methanolic supercritical fluid extract of *Platanus occidentalis* L. (Platanaceae), the American sycamore. The structures of these metabolites were determined to be kaempferol 3-*O*-α-L-(2″,3″-di-*E*-*p*-coumaroyl)rhamnoside (**10**), kaempferol 3-*O*-α-L-(2″-*E*-*p*-coumaroyl-3″-*Z*-*p*-coumaroyl)rhamnoside (**11**), kaempferol 3-*O*-α-L-(2″-*Z*-*p*-coumaroyl-3″-*E*-*p*-coumaroyl)-rhamnoside (**12**), and kaempferol 3-*O*-α-L-(2″,3″-di-*Z*-*p*-coumaroyl)rhamnoside (**13**) based on analysis of their NMR and HRESIMS data and by comparing these values with data reported for these compounds.[17] The metabolites exhibited inhibitory activities against the drug-sensitive parasites with IC_{50} values ranging from 0.5 to 2.0 μM (Table 3). Among the kaempferol 3-*O*-rhamnosides, compound **10** showed the best selectivity for malaria compared to human cells, but the compounds were less potent against the drug-resistant malaria line (Table 3). This resulted in selectivity values of less than 4-fold for the drug-resistant malaria strains compared to human cells.

Additionally, four known kaempferol 3-*O*-glycosides (**14**−**17**) were purified from the methanolic supercritical fluid extract of the Lacey oak (*Quercus laceyi* Small, Fagaceae). The structures of the flavonoid glycosides were determined to be kaempferol-3-*O*-(3″,4″-diacetyl-2″,6″-di-*E*-*p*-coumaroyl)-glucoside (**14**),[18] kaempferol 3-*O*-(2″-*cis*-*p*-coumaroyl-3″,4″-diacetyl-6″-*trans*-*p*-coumaroyl)-β-D-glucopyranoside (**15**),[19] kaempferol-3-*O*-(2″-*trans*-*p*-coumaroyl-3″, 4″-diacetyl-6″-*cis*-*p*-coumaroyl)-β-D-glucopyranoside (**16**),[20] and kaempferol-3-*O*-(3″,4″-diacetyl-2″,6″-di-*Z*-*p*-coumaroyl)glucoside (**17**),[18] based on comparisons with published data. Compounds **14**−**17** exhibited IC_{50} values in the range 0.6−2.1 μM against the drug-sensitive parasite, but were 2 to 5 times less potent against the drug-resistant strain and showed no selectivity for the parasite compared to human cells (Table 3). While there has been some effort to explore flavonoids as antimalarial agents,[6] members of this class have been reported to exhibit a wide variety of biological activities due to their proclivities for nonspecific inhibition of various biological targets.[27,28] This is consistent with their less than 5-fold selectivity for malaria as compared to HeLa cells in our assay, making them less than ideal candidates for further investigation.

The aqueous extract of *Bulbine frutescens* Willd. (Asphodelaceae) yielded the known compound knipholone.[14] The active compound was identified by 96-well microtiter plate fractionation of the extract, which generated a single bioactive well. Dereplication was performed based on taxonomic considerations, as well as the metabolite's UV-PDA profile and MS data.[14] Scale-up processing of the crude extract over silica gel, HP20ss, and C_{18} HPLC yielded several milligrams of the pure metabolite, which enabled the confirmation of its structure by NMR spectroscopy. Knipholone exhibited an IC_{50} of 4.9 μM against the drug-sensitive HB3 parasite and almost identical potency against the NHP1337 drug-resistant parasite (Table 3). This is consistent with the reported activity of knipholone against both drug-sensitive and -resistant parasites.[29] Additionally, knipholone showed greater than 6-fold selective activity against the parasite versus HeLa cells (Table 3), which is also consistent with published results.[29]

Another known compound, amentoflavone,[15] was obtained from the methanolic supercritical fluid extract of the evergreen sumac, *Rhus virens* Lindheim ex A. Gray (Anacardiaceae). Amentoflavone was previously demonstrated to have a wide range of biological activities and was identified in a large-scale screen for inhibitors of the M1 family of alanyl aminopeptidases in *P. falciparum*.[30] In the current study, it was determined that amentoflavone exhibited relatively weak activity against both drug-sensitive and -resistant parasites and was only 2-fold more selective toward *P. falciparum* compared to its activity against HeLa cells (Table 3).

EXPERIMENTAL SECTION

General Experimental Procedures. Optical rotation data were determined on a Rudolph Research AUTOPOL III automatic polarimeter. IR data were collected on a Shimadzu IR Affinity FTIR. UV data were collected on a Hewlett-Packard 8452A diode array spectrophotometer. NMR data were collected on Varian 400 and 500 MHz NMR spectrometers. Accurate mass data were collected on an Agilent 6538 HRESI QTOF MS coupled to an Agilent 1290 HPLC. LCESIMS data were obtained on a Shimadzu LC-MS 2020 system (ESI quadrupole) coupled to a photodiode array detector, with a Phenomenex Kintex column (2.6 μm C_{18} column, 100 Å, 75 × 3.0 mm). The preparative HPLC system utilized SCL-10A VP pumps and system controller with a Luna 5 μm C_{18} column (110 Å, 250 × 21.2 mm, 10 mL/min), and the analytical and semipreparative HPLC system utilized Waters 1525 binary pumps with Waters 2998 photodiode array detectors and Luna 5 μm C_{18} columns (110 Å, 250 × 4.6 mm, 1 mL/min and 110 Å, 250 × 10 mm, 4 mL/min). X-ray data were collected using a diffractometer with a Bruker APEX CCD area detector and graphite-monochromated Mo Kα radiation (λ = 0.710 73 Å). All solvents were of ACS grade or better.

For each experiment, a sample of 20 mg of crude plant extract was dissolved in 2 mL of HPLC grade MeOH, and the suspension was centrifuged. The supernatant was passed over HP20ss and C_{18} silica gel columns (both eluted with MeOH), and the residue resuspended to yield a 50 mg/mL solution in HPLC grade MeOH. A 100 μL

DOI: 10.1021/acs.jnatprod.5b00874
J. Nat. Prod. XXXX, XXX, XXX−XXX

aliquot (5 mg of soluble plant extract material) was loaded onto a C_{18} semipreparative HPLC column, and fractions were collected in a deep-well 96-well plate. HPLC separations were performed under gradient conditions progressing from 30:70 MeOH–H_2O to 100% MeOH in 30 min, followed by a column wash with 100% MeOH for another 10 min. The resulting microtiter plate contained 92 wells, which were each filled with 1.7 mL of eluent. The contents of each well were split into two plates, and the solvent was removed under vacuum. For bioassay analysis, the contents in each well of one plate were resuspended in DMSO for testing, whereas the contents of the second matched plate were retained for follow-up LCESIMS analysis of the bioactive components.

Plant Material. The leaves and stems of *Bulbine frutescens* (bulbine) and *Buxus sempervirens* (the common boxwood) were collected from the San Antonio Botanical Garden (SABG) in June 2005. The leaves and stems of *Rhus virens* (the evergreen sumac) were obtained from Natives of Texas Nursery in March 2007. The leaves and stems of *Platanus occidentalis* (the American sycamore) and *Quercus laceyi* (the Lacey oak) were collected from the SABG in April 2014. Additional re-collections of plant material were obtained from SABG or local plant nurseries (Casa Verde, Hill Country African Violets). Voucher specimens of *Bulbine frutescens* (SLM223), *Buxus sempervirens* (SLM245), *Rhus virens* (SLM316), *Platanus occidentalis* (SLM2047), and *Quercus laceyi* (SLM2046) were made and stored in the Mooberry laboratory herbarium at UTHSCSA. The remaining plant materials were rapidly frozen to preserve their chemical integrity prior to freeze-drying. Half of the plant material was used to generate two lipophilic extracts by supercritical fluid extraction. The first lipophilic extract was generated using CO_2 only, which was followed by a second extraction with methanol and CO_2 to yield a less hydrophobic extract. The other half of the plant material was extracted using 70% H_2O and 30% EtOH to generate an aqueous extract.

Extraction and Isolation. The methanolic supercritical fluid extract (2.5 g) of *Buxus sempervirens* was fractionated over silica gel and eluted with hexane–CH_2Cl_2–MeOH (hexane, 50:50 hexane–CH_2Cl_2, CH_2Cl_2, 90:10 CH_2Cl_2–MeOH, MeOH). Fractions 4 and 5 were combined, applied to an HP20ss column, and eluted with MeOH–H_2O. The fourth fraction (MeOH–H_2O, 90:10) was further separated over Sephadex LH20 (eluted with MeOH) to yield five subfractions. Subfraction 3 was separated by C_{18} preparative HPLC (gradient elution with MeOH–H_2O from 30:70 to 100% organic phase in 30 min) followed by C_{18} semipreparative HPLC (MeCN–H_2O, 75:25) to obtain **1** (15.0 mg), **2** (5.5 mg), **3** (0.9 mg), and **4** (1.2 mg, isomerized to a ~3:1 mixture of **4** and **3**). Compounds from the Sephadex-LH20-derived subfraction 4 were further purified by C_{18} preparative HPLC (MeOH–H_2O gradient from 30:70 to 100% organic phase in 30 min) and C_{18} semipreparative HPLC (MeCN–H_2O, 75:25) to yield **5** (8.4 mg) (this isomerized into a 4:1 mixture of **5** and **6**), **6** (15.4 mg) (this also isomerized over time into a mixture of **5** and **6**), and a 2:1 mixture of **7** and **8** (1.4 mg).

*23-O-(Z)-p-Coumaroyl-23-hydroxybetulin (**1**):* colorless, block-shaped crystals; $[\alpha]^{20}_D$ +80.9 (*c* 0.21, MeOH); UV (MeOH) λ_{max} (log ε) 208 (4.49), 310 (4.31) nm; IR (film) ν_{max} 2931, 2864, 1739, 1689, 1541, 1514, 1454, 1161; ^{1}H and ^{13}C NMR, see Tables 1 and 2; HRESIMS $[M - H]^-$ *m*/*z* 603.4066 (calcd for $C_{39}H_{55}O_5$, 603.4055).

*23-O-(E)-p-Coumaroyl-23-hydroxybetulin (**2**):* white, amorphous powder; $[\alpha]^{20}_D$ −3.6 (*c* 0.45, MeOH); UV (MeOH) λ_{max} (log ε) 208 (4.05), 314 (4.25) nm; IR (film) ν_{max} 2937, 2868, 1739, 1689, 1541, 1514, 1454, 1165 cm^{-1}; ^{1}H and ^{13}C NMR, see Table S1, Supporting Information; HRESIMS $[M - H]^-$ *m*/*z* 603.4078 (calcd for $C_{39}H_{55}O_5$, 603.4055).

*23-O-(trans)-Feruloyl-23-hydroxybetulin (**3**):* white, amorphous powder; $[\alpha]^{20}_D$ +8.9 (*c* 0.045, MeOH); UV (MeOH) λ_{max} (log ε) 206 (4.09), 326 (4.07) nm; IR (film) ν_{max} 3437, 2941, 2868, 1641, 1514, 1454, 1392, 1263, 1159, 1018 cm^{-1}; ^{1}H and ^{13}C NMR, see Tables 1 and 2; HRESIMS $[M - H]^-$ *m*/*z* 633.4178 (calcd for $C_{40}H_{57}O_6$, 633.4161).

*23-O-(cis)-Feruloyl-23-hydroxybetulin and 23-O-(trans)-feruloyl-23-hydroxybetulin (mixture of **4** and **3**, ~3:1 ratio):* white, amorphous powder; $[\alpha]^{20}_D$ +86.2 (*c* 0.065, MeOH); UV (MeOH) λ_{max} (log ε) 206 (4.05), 326 (4.03) nm; IR (film) ν_{max} 2935, 2866, 1739, 1689, 1541, 1514, 1454, 1265 cm^{-1}; ^{1}H and ^{13}C NMR, see Tables 1 and 2; HRESIMS $[M - H]^-$ *m*/*z* 633.4162 (calcd for $C_{40}H_{57}O_6$, 633.4161).

*3-O-(cis)-p-Coumaroyl-23-hydroxybetulin and 3-O-(E)-p-coumaroyl-23-hydroxybetulin (mixture of **5** and **6**, ~4:1):* white, amorphous powder; $[\alpha]^{20}_D$ +27.4 (*c* 0.18, MeOH); UV (MeOH) λ_{max} (log ε) 208 (4.09), 312 (4.16) nm; IR (film) ν_{max} 3415, 2943, 2870, 1641, 1512, 1392, 1165, 1016 cm^{-1}; ^{1}H and ^{13}C NMR, see Tables 1 and 2; HRESIMS $[M - H]^-$ *m*/*z* 603.4074 (calcd for $C_{39}H_{55}O_5$, 603.4055).

*3-O-(E)-p-Coumaroyl-23-hydroxybetulin (**6**):* white, amorphous powder; $[\alpha]^{20}_D$ +24.8 (*c* 0.25, $CHCl_3$–MeOH, 1:1); UV (MeOH) λ_{max} (log ε) 208 (3.98), 310 (4.21) nm; IR (film) ν_{max} 2935, 1687, 1539, 1514, 1419, 1394, 1157 cm^{-1}; ^{1}H and ^{13}C NMR, see Table S1, Supporting Information; HRESIMS $[M - H]^-$ *m*/*z* 603.4062 (calcd for $C_{39}H_{55}O_5$, 603.4055).

*3-O-(trans)-Feruloyl-23-hydroxybetulin and 3-O-(cis)-feruloyl-23-hydroxybetulin (mixture of **7** and **8**, ~2:1):* white, amorphous powder; $[\alpha]^{20}_D$ +22.9 (*c* 0.07, MeOH); UV (MeOH) λ_{max} (log ε) 206 (4.10), 326 (4.10) nm; IR (film) ν_{max} 2937, 2870, 1678, 1539, 1454, 1269, 1178 cm^{-1}; ^{1}H and ^{13}C NMR, see Tables 1 and 2; HRESIMS $[M - H]^-$ *m*/*z* 633.4178 (calcd for $C_{40}H_{57}O_6$, 633.4161).

*23-Hydroxybetulin (**9**):* A 0.5 mL amount of 1 M NaOH was added to 23-*O*-(*Z*)-*p*-coumaroyl-23-hydroxybetulin (**1**) (5.0 mg), and the system was stirred overnight at room temperature. A saturated aqueous solution of NaCl (2 mL) was added to this mixture and was further partitioned with EtOAc. The organic phase was evaporated under reduced pressure. 23-Hydroxybetulin (**9**) (3 mg) was obtained after further purification by semipreparative HPLC: white, amorphous powder; $[\alpha]^{20}_D$ +16.0 (*c* 0.2, $CHCl_3$). ESIMS $[M - H_2O + H]^+$ *m*/*z* 441, $[M - 2H_2O + H]^+$ *m*/*z* 423, $[M + HCOOH - H]^-$ *m*/*z* 503; ^{1}H and ^{13}C NMR, see Figures S45 and S46, Supporting Information.

The methanolic supercritical extract (1.67 g) of *Platanus occidentalis* was fractionated by HP20ss column chromatography (eluted with MeOH–H_2O). Fraction 4 was processed by C_{18} preparative HPLC (MeOH–H_2O gradient from 30:70 to 100% organic phase over 30 min) and C_{18} semipreparative HPLC (MeCN–H_2O, 50:50) to yield **10** (3.0 mg), **11** (1.2 mg), **12** (1.0 mg), and **13** (0.8 mg). The methanolic supercritical extract (0.95 g) of *Quercus laceyi* was fractionated by HP20ss column chromatography (eluted with MeOH–H_2O). Fraction 4 (MeOH–H_2O, 90:10) was processed by C_{18} preparative HPLC (with a MeOH–H_2O gradient from 30:70 to 100% organic over 30 min) and C_{18} semipreparative HPLC (MeCN–H_2O, 47.5:52.5) to yield **14** (2.0 mg), **15** (1.0 mg), **16** (1.0 mg), and **17** (0.5 mg). The aqueous extract (0.5 g) of *Bulbine fruticosa* was fractionated over silica gel (eluted with hexane–CH_2Cl_2–MeOH). Fraction 4 was passed over an HP20ss column and eluted with MeOH–H_2O. Subfraction 4 was further processed by C_{18} preparative HPLC (MeOH–H_2O gradient from 30:70 to 100% organic phase in 30 min) and C_{18} semipreparative HPLC (isocratic 50:50 MeOH–H_2O) to yield knipholone (3.0 mg). The supercritical/MeOH extract (4.88 g) of *Rhus virens* was subjected to fractionation by silica flash chromatography (gradient elution with CH_2Cl_2–MeOH). The fraction eluting with 20:80 MeOH–H_2O was further purified by preparative HPLC using a Phenomenex C_{18} column with a MeCN–H_2O gradient from 20:80 to 80:20 in 50 min to yield amentoflavone. The biological activities of amentoflavone were found to be identical with a commercially obtained sample of amentoflavone from Sigma-Aldrich (St. Louis, MO, USA).

X-ray Crystal Structure Analysis of 23-*O*-(*Z*)-*p*-Coumaroyl-23-hydroxybetulin (1). A colorless, block-shaped crystal of dimensions 0.420 × 0.220 × 0.090 mm was selected for structural analysis. Intensity data for this compound were collected using a diffractometer with a Bruker APEX CCD area detector[31] and graphite-monochromated Mo Kα radiation (λ = 0.710 73 Å). The sample was cooled to 100(2) K. Cell parameters were determined from a nonlinear least-squares fit of 8005 peaks in the range 2.45° < θ < 26.91°. A total of 27 638 data were measured in the range 1.832° < θ < 26.920° using φ and ω oscillation frames. The data were corrected for

DOI: 10.1021/acs.jnatprod.5b00874
J. Nat. Prod. XXXX, XXX, XXX–XXX

absorption by the empirical method,[32] giving minimum and maximum transmission factors of 0.969 and 0.993. The data were merged to form a set of 7493 independent data with $R(\mathrm{int}) = 0.0325$ and a coverage of 100.0%. The orthorhombic space group $P2_12_12_1$ was determined by systematic absences and statistical tests and verified by subsequent refinement. The structure was solved by direct methods and refined by full-matrix least-squares methods on F^2.[33] The positions of hydrogens bonded to carbons were initially determined by geometry and were refined using a riding model. Hydrogens bonded to oxygens were located on a difference map, and their positions were refined independently. Non-hydrogen atoms were refined with anisotropic displacement parameters. Hydrogen atom displacement parameters were set to 1.2 (1.5 for methyl) times the isotropic equivalent displacement parameters of the bonded atoms. A total of 406 parameters were refined against 7493 data to give $wR(F^2) = 0.1081$ and $S = 0.994$ for weights of $w = 1/[\sigma^2(F^2) + (0.0600P)^2 + 0.6000P]$, where $P = [F_o^2 + 2F_c^2]/3$. The final $R(F)$ was 0.0421 for the 6343 observed, $[F > 4\sigma(F)]$, data. The largest shift/s.u. was 0.000 in the final refinement cycle. The final difference map had maxima and minima of 0.257 and −0.161 e/Å^3, respectively. The absolute structure was determined by refinement of the Hooft parameter[21] [Hooft $y = 0.3(4)$, $P2(\mathrm{true}) = 0.831$, $P3(\mathrm{true}) = 0.455$, $P3(\mathrm{false}) = 0.093$, $P3(\mathrm{rac\text{-}twin}) = 0.453$]. The X-ray crystallographic data for **1** have been deposited with the Cambridge Crystallographic Data Center under accession number CCDC 1420620. The data can be accessed free of charge at http://www.ccdc.cam.ac.uk.

Malarial Parasite Inhibition Assays. Samples were evaluated for their abilities to inhibit the growth of malaria parasites using a SYBR green-based assay.[34] Briefly, an aliquot of plant extract was added to 100 μL of *P. falciparum* cell culture containing ring stage parasites at 0.5% parasitemia. Test plates were maintained at 37 °C under standard parasite culture conditions for 72 h, at which time parasite growth was measured. Each plate contained positive controls to measure uninhibited parasite growth and negative controls consisting of uninfected red blood cells to measure background fluorescence. The percent inhibition was calculated as the reduction in SYBR fluorescence measured in the presence of plant extract relative to the positive control. Selective extracts were evaluated a second time to verify their antimalarial activity and specificity. The relative potencies of the purified compounds were determined by running full dose−response curves over concentration ranges covering 3 orders of magnitude. The IC_{50} values were calculated from the dose−response curves.

Initial screening of crude plant extracts was conducted with a laboratory parasite (HB3) that is sensitive to antimalarials (chloroquine, antifolates, mefloquine, quinine, and artemisinin). Purified compounds showing activity against HB3 were further tested using a parasite clone recently isolated from the Thailand−Myanmar border. This parasite is multi-drug-resistant, and its collection was approved by the ethics review boards of the Faculty of Tropical Medicine, Mahidol University, Thailand. The genome has mutations encoding chloroquine resistance (chloroquine resistance transporter (*pfcrt*) K76T) and artemisinin resistance (kelch-C580Y). Antifolate resistance was also expected since parasites from this region are generally resistant to antifolate drugs due to combinations of mutations in both the dihydrofolate reductase (*dhfr*) and dihydropteroate synthase genes (*dhps*).[35] Furthermore, this parasite was isolated from a patient showing slow parasite clearance following artemisinin combination therapy, providing further confirmation of artemisinin resistance.

HeLa Cell Line Counterscreen. Each of the plant extracts and purified compounds that exhibited antimalarial activity was evaluated against the HeLa human cervical cancer cell line as a first step to evaluate specificity for malaria versus nonspecific toxicity. HeLa cells were obtained from the American Type Culture Collection (Manassas, VA, USA) and cultured in Basal Medium Eagle with Earle's salts (Sigma-Aldrich) with 10% fetal bovine serum and 50 μg/mL gentamicin. The sulforhodamine B assay was used to measure antiproliferative and cytotoxic activities as previously described.[36,37]

■ ASSOCIATED CONTENT

Ⓢ Supporting Information

The Supporting Information is available free of charge on the ACS Publications website at DOI: 10.1021/acs.jnatprod.5b00874.

Summaries of 2D NMR correlation data, 1D and 2D NMR spectra, and HRESIMS data (PDF)

■ AUTHOR INFORMATION

Corresponding Authors

*Phone: 210-567-4788. Fax: 210-567-4300. E-mail: mooberry@uthscsa.edu.

*Phone: 405-325-6969. Fax: 405-325-6111. E-mail: rhcichewicz@ou.edu.

Author Contributions

#S. Cai and A. L. Risinger contributed equally to this work.

Notes

The authors declare no competing financial interest.

■ ACKNOWLEDGMENTS

Support for this project was provided by a pilot studies grant from the Texas Biomedical Forum and R21AI092235 awarded to S.L.M. and T.J.C.A. from the National Institute for Allergy and Infectious Disease, National Institutes of Health (NIH), Bethesda, MD. This investigation was conducted in facilities constructed with support from Research Facilities Improvement Program grants C06 RR013556 and RR017515 from the National Center for Research Resources of the NIH. Parasite clone NHP1337 was isolated from an infected blood sample collected on the Thailand−Myanmar border provided by F. Nosten. T.J.C.A. and S.N. are supported by grant R37AI048071 from the National Institute of Allergy and Infectious Diseases. The LC-MS instrument used for this project was provided in part by a Challenge Grant from the Office of the Vice President for Research, University of Oklahoma, Norman Campus, and an award through the Shimadzu Equipment Grant Program (R.H.C.). We thank A. Robles and L. Clark for their assistance in plant collections and extractions and the San Antonio Botanical Garden for access to plant samples.

■ DEDICATION

Dedicated to Professors John Blunt and Murray Munro, of the University of Canterbury, for their pioneering work on bioactive marine natural products.

■ REFERENCES

(1) World Health Organization. Fact Sheet No. 94, 2015. http://www.who.int/mediacentre/factsheets/fs094/en/ (accessed Oct 1, 2015).

(2) Hayton, K.; Su, X. Z. *Curr. Drug Targets: Infect. Disord.* **2004**, *4*, 1−10.

(3) (a) Ashley, E. A.; Dhorda, M.; Fairhurst, R. M.; Amaratunga, C.; Lim, P.; Suon, S.; Sreng, S.; Anderson, J. M.; Mao, S.; Sam, B.; Sopha, C.; Chuor, C. M.; Nguon, C.; Sovannaroth, S.; Pukrittayakamee, S.; Jittamala, P.; Chotivanich, K.; Chutasmit, K.; Suchatsoonthorn, C.; Runcharoen, R.; Hien, T. T.; Thuy-Nhien, N. T.; Thanh, N. V.; Phu, N. H.; Htut, Y.; Han, K. T.; Aye, K. H.; Mokuolu, O. A.; Olaosebikan, R. R.; Folaranmi, O. O.; Mayxay, M.; Khanthavong, M.; Hongvanthong, B.; Newton, P. N.; Onyamboko, M. A.; Fanello, C. I.; Tshefu, A. K.; Mishra, N.; Valecha, N.; Phyo, A. P.; Nosten, F.; Yi, P.; Tripura, R.; Borrmann, S.; Bashraheil, M.; Peshu, J.; Faiz, M. A.; Ghose, A.; Hossain, M. A.; Samad, R.; Rahman, M. R.; Hasan, M. M.; Islam, A.; Miotto, O.; Amato, R.; MacInnis, B.; Stalker, J.;

DOI: 10.1021/acs.jnatprod.5b00874
J. Nat. Prod. XXXX, XXX, XXX−XXX

Kwiatkowski, D. P.; Bozdech, Z.; Jeeyapant, A.; Cheah, P. Y.; Sakulthaew, T.; Chalk, J.; Intharabut, B.; Silamut, K.; Lee, S. J.; Vihokhern, B.; Kunasol, C.; Imwong, M.; Tarning, J.; Taylor, W. J.; Yeung, S.; Woodrow, C. J.; Flegg, J. A.; Das, D.; Smith, J.; Venkatesan, M.; Plowe, C. V.; Stepniewska, K.; Guerin, P. J.; Dondorp, A. M.; Day, N. P.; White, N. J. *N. Engl. J. Med.* **2014**, *371*, 411−423. (b) Fidock, D. A.; Eastman, R. T.; Ward, S. A.; Meshnick, S. R. *Trends Parasitol.* **2008**, *24*, 537−544.

(4) White, N. J. *Science* **2008**, *320*, 330−334.

(5) Onguéné, P. A.; Ntie-Kang, F.; Lifongo, L. L.; Ndom, J. C.; Sippl, W.; Mbaze, L. M. *Malar. J.* **2013**, *12*, 449.

(6) Ntie-Kang, F.; Onguéné, P. A.; Lifongo, L. L.; Ndom, J. C.; Sippl, W.; Mbaze, L. M. *Malar. J.* **2014**, *13*, 81.

(7) Meshnick, S. R.; Taylor, T. E.; Kamchonwongpaisan, S. *Microbiol. Rev.* **1996**, *60*, 301−315.

(8) White, N. J.; Nosten, F.; Looareesuwan, S.; Watkins, W. M.; Marsh, K.; Snow, R. W.; Kokwaro, G.; Ouma, J.; Hien, T. T.; Molyneux, M. E.; Taylor, T. E.; Newbold, C. I.; Ruebush, T. K.; Danis, M.; Greenwood, B. M.; Anderson, R. M.; Olliaro, P. *Lancet* **1999**, *353*, 1965−1967.

(9) Carraz, M.; Jossang, A.; Franetich, J. F.; Siau, A.; Ciceron, L.; Hannoun, L.; Sauerwein, R.; Frappier, F.; Rasoanaivo, P.; Snounou, G.; Mazier, D. *PLoS Med.* **2006**, *3*, e513.

(10) Oliveira, A. B.; Dolabela, M. F.; Braga, F. C.; Jacome, R. L.; Varotti, F. P.; Povoa, M. M. *An. Acad. Bras. Cienc.* **2009**, *81*, 715−740.

(11) Rasoanaivo, P.; Ramanitrahasimbola, D.; Rafatro, H.; Rakotondramanana, D.; Robijaona, B.; Rakotozafy, A.; Ratsimamanga-Urverg, S.; Labaied, M.; Grellier, P.; Allorge, L.; Mambu, L.; Frappier, F. *Phytother. Res.* **2004**, *18*, 742−747.

(12) http://www.srh.noaa.gov/crp/?n=localclimate (accessed Oct 1, 2015).

(13) Williams, R. B.; Gutekunst, W. R.; Joyner, P. M.; Du, W.; Li, Q.; Ross, C. A.; Williams, T. D.; Cichewicz, R. H. *J. Agric. Food Chem.* **2007**, *55*, 9450−9456.

(14) van Staden, L. F.; Drewes, S. E. *Phytochemistry* **1993**, *35*, 685−686.

(15) Markham, K. R.; Sheppard, C.; Geiger, H. *Phytochemistry* **1987**, *26*, 3335−3337.

(16) Pan, L.; Muñoz Acuña, U.; Chai, H.; Park, H. Y.; Ninh, T. N.; Thanh, B. V.; Merino, E. F.; Cassera, M. B.; Rakotondraibe, L. H.; Carcache de Blanco, E. J.; Soejarto, D. D.; Kinghorn, A. D. *Planta Med.* **2015**, *81*, 1133−1140.

(17) Ibrahim, M. A.; Mansoor, A. A.; Gross, A.; Ashfaq, M. K.; Jacob, M.; Khan, S. I.; Hamann, M. T. *J. Nat. Prod.* **2009**, *72*, 2141−2144.

(18) Karioti, A.; Bilia, A. R.; Skaltsa, H. *Food Chem.* **2010**, *123*, 131−142.

(19) Meng, Z.; Zhou, Y.; Lu, J.; Sugahara, K.; Xu, S.; Kodama, H. *Clin. Chim. Acta* **2001**, *306*, 97−102.

(20) Wang, L.; Jiang, M.; Xu, S.; Sun, Q.; Zeng, G.; Zhou, Y. *Nat. Prod. Commun.* **2010**, *5*, 1597−1599.

(21) Hooft, R. W. W.; Straver, L. H.; Spek, A. L. *J. Appl. Crystallogr.* **2008**, *41*, 96−103.

(22) Dračínský, M.; Richtr, V.; Křeček, V.; Sejbal, J.; Klinot, J.; Buděšínský, M. *Collect. Czech. Chem. Commun.* **2006**, *71*, 387−410.

(23) Becke, D. *J. Chem. Phys.* **1993**, *98*, 5648−5652.

(24) Frisch, M. J.; Trucks, G. W.; Schlegel, H. B.; Scuseria, G. E.; Robb, M. A.; Cheeseman, J. R.; Scalmani, G.; Barone, V.; Mennucci, B.; Petersson, G. A.; Nakatsuji, H.; Caricato, M.; Li, X.; Hratchian, H. P.; Izmaylov, A. F.; Bloino, J.; Zheng, G.; Sonnenberg, J. L.; Hada, M.; Ehara, M.; Toyota, K.; Fukuda, R.; Hasegawa, J.; Ishida, M.; Nakajima, T.; Honda, Y.; Kitao, O.; Nakai, H.; Vreven, T.; Montgomery, J. A., Jr.; Peralta, J. E.; Ogliaro, F.; Bearpark, M.; Heyd, J. J.; Brothers, E.; Kudin, K. N.; Staroverov, V. N.; Kobayashi, R.; Normand, J.; Raghavachari, K.; Rendell, A.; Burant, J. C.; Iyengar, S. S.; Tomasi, J.; Cossi, M.; Rega, N.; Millam, J. M.; Klene, M.; Knox, J. E.; Cross, J. B.; Bakken, V.; Adamo, C.; Jaramillo, J.; Gomperts, R.; Stratmann, R. E.; Yazyev, O.; Austin, A. J.; Cammi, R.; Pomelli, C.; Ochterski, J. W.; Martin, R. L.; Morokuma, K.; Zakrzewski, V. G.; Voth, G. A.; Salvador, P.; Dannenberg, J. J.; Dapprich, S.; Daniels, A. D.; Farkas, Ö.; Foresman, J. B.; Ortiz, J. V.; Cioslowski, J.; Fox, D. J. *Gaussian 09*, Revision A.1; Gaussian, Inc.: Wallingford, CT, 2009.

(25) Liu, Y.; Kubo, M.; Fukuyama, Y. *J. Nat. Prod.* **2012**, *75*, 1353−1358.

(26) Ye, M.; Xiong, J.; Zhu, J.; Hong, J.; Zhao, Y.; Fan, H.; Yang, G.; Xia, G.; Hu, J. *J. Nat. Prod.* **2014**, *77*, 178−182.

(27) Duan, D.; Doak, A. K.; Nedyalkova, L.; Shoichet, B. K. *ACS Chem. Biol.* **2015**, *10*, 978−988.

(28) Ingolfsson, H. I.; Thakur, P.; Herold, K. F.; Hobart, E. A.; Ramsey, N. B.; Periole, X.; de Jong, D. H.; Zwama, M.; Yilmaz, D.; Hall, K.; Maretzky, T.; Hemmings, H. C., Jr.; Blobel, C.; Marrink, S. J.; Kocer, A.; Sack, J. T.; Andersen, O. S. *ACS Chem. Biol.* **2014**, *9*, 1788−1798.

(29) Bringmann, G.; Menche, D.; Bezabih, M.; Abegaz, B. M.; Kaminsky, R. *Planta Med.* **1999**, *65*, 757−758.

(30) http://pubchem.ncbi.nlm.nih.gov/assay/assay.cgi?aid=1445 (accessed Oct 1, 2015).

(31) (a) Data collection: *APEX2*; Bruker AXS Inc., Madison, WI, USA, 2007. (b) Data reduction: *SAINT*; Bruker AXS Inc.: Madison, WI, USA, 2007.

(32) Krause, L.; Herbst-Irmer, R.; Sheldrick, G. M.; Stalke, D. *J. Appl. Crystallogr.* **2015**, *48*, 3−10.

(33) (a) Sheldrick, G. M. *Acta Crystallogr., Sect. A: Found. Adv.* **2015**, *A71*, 3−8. (b) Sheldrick, G. M. *Acta Crystallogr.* **2015**, *C71*, 3−8.

(34) Johnson, J. D.; Dennull, R. A.; Gerena, L.; Lopez-Sanchez, M.; Roncal, N. E.; Waters, N. C. *Antimicrob. Agents Chemother.* **2007**, *51*, 1926−1933.

(35) Nair, S.; Brockman, A.; Paiphun, L.; Nosten, F.; Anderson, T. J. *Int. J. Parasitol.* **2002**, *32*, 852−858.

(36) Skehan, P.; Storeng, R.; Scudiero, D.; Monks, A.; McMahon, J.; Vistica, D.; Warren, J. T.; Bokesch, H.; Kenney, S.; Boyd, M. R. *J. Natl. Cancer Inst.* **1990**, *82*, 1107−1112.

(37) Vichai, V.; Kirtikara, K. *Nat. Protoc.* **2006**, *1*, 1112−1116.

DOI: 10.1021/acs.jnatprod.5b00874
J. Nat. Prod. XXXX, XXX, XXX−XXX